

# A Numerical Analysis of NMR Pore-Pore Exchange Measurements using Micro X-ray Computed Tomography

*Y. Melean,<sup>1,2</sup> K.E. Washburn,<sup>3,4</sup> P.T. Callaghan,<sup>3</sup> C.H. Arns<sup>1,2</sup>*

<sup>1</sup> School of Petroleum Engineering, University of New South Wales, Australia

<sup>2</sup> Dept. of Applied Mathematics, Australian National University

<sup>3</sup> School of Chemical and Physical Sciences, Victoria University Wellington, NZ

<sup>4</sup> ResLab, Reservoir Laboratories AS, Trondheim, Norway

Corresponding author: Christoph Arns, E-Mail: c.arns@unsw.edu.au

(received 14 July 2008, accepted 11 June 2009)

## Abstract

Pore-pore relaxation exchange experiments are a recent development and hold great promise to spectrally derive length scales and connectivity information relevant for transport in porous media. However, for large pores, NMR diffusion-relaxation techniques reach a limit because bulk relaxation becomes dominant. A combination of NMR and Xray-CT techniques could be beneficial and lead to better models for regions of unresolved porosity in CT images, increasing the accuracy of image based calculations of transport properties. In this study we carry out numerical NMR pore-pore exchange experiments on selected Xray-CT images of sandstones and carbonate rock, while at the same time tracking information about the geometry and topology of the pore space. We use pore partitioning techniques and geometric distance fields to relate  $T_2$ - $T_2$  relaxation exchange spectra to underlying structural quantities. It is shown that  $T_2$ - $T_2$  pore-pore exchange measurements at room temperatures for the samples considered likely reflect exchange between pores and throats or pores and roughness.

## Keywords

NMR relaxation, exchange, porous media, micro X-ray CT, order parameters

## 1. Introduction

The measurement of structural length scales of the pore space of porous media by NMR techniques has a long tradition [1-5]. Usually, NMR relaxation techniques are employed, which however e.g. for rocks are only applicable if a series of assumptions hold, in particular constant surface relaxivity, the weak coupling limit, and fast diffusion [6,7]. Recently, a technique relaxing some of these assumptions has been presented [8-11], using 2D NMR relaxation exchange measurements. However, cross-peaks between small and large relaxation times could be caused by either exchange between small and large pores, pores and constrictions, or regions initially away from a surface and surface crevices/regions.

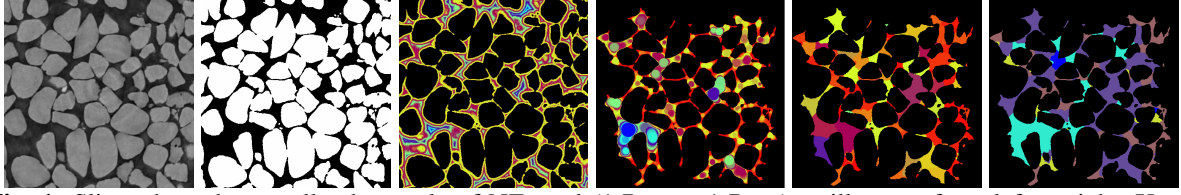


**Fig. 1:** Slices through a small sub-sample of NZ sand (1.7mm x 1.7mm) to illustrate from left to right: X-ray density map, segmented image, Euclidean distance map, covering radius map, and pore partitions. For the two pore partitions (right) colours are assigned by equivalent sphere radius reflecting volume and volume/surface ratio.

From Xray-CT images both pore size and connectivity are directly measurable. Previously we considered the morphological characteristics of reservoir rocks [12], cross-correlations of morphology and transport properties [13,14], and analysed 1D NMR relaxation responses [15,16]. In this work we extend the analysis to 2D NMR relaxation exchange experiments.

## 2. Methods and Results

All rock samples considered in this study were acquired on the ANU micro-CT facility [17,18]. This study is based on the resulting binary images, partitions derived thereof, and diffusion-relaxation weighted measures derived from these partitions (see Fig. 1).

### 2.1. Pore Space Partitions

We consider two distance maps. The Euclidean distance map (EDM) assigns each voxel of the pore space the shortest distance to the solid surface. Each voxel of the covering radius map (CRM) reflects the radius of the largest sphere which is contained in the pore space and covers the voxel. The CRM thus assigns small radii to small pores, constrictions between pores, and surface roughness. In addition to the distance maps we partition the void space into simple geometric cells (pores) separated by constriction surfaces [15].

### 2.2. Spatial-Temporal Averages

Based on the partitions we define length scales as either sphere diameters directly derived from the distance maps ( $d_{EDM}$ ,  $d_{CRM}$ ), or as equivalent sphere diameters from the pores of the pore partition, using equivalent volume  $V$ ,  $d_v = 2(3V)^{1/3}(4\pi)^{-1/3}$ , or equivalent structural length  $d_{vs} = 6V/S$ , where  $S$  is the surface area of the pore. We then carry out a random walk simulation for a  $T_2$ - $T_2$  exchange experiment, using encoding time  $t_E$  and diffusion time  $t_D$ . These distance measures and relaxation rates are averaged for each of the two encoding intervals, resulting in exchange plots for each of the measures. Relaxation rates are set either on distance basis (coarse scale, e.g.  $T_{2CRT}$ ), or on voxel scale (standard  $T_2$ - $T_2$  simulation, using bulk- relaxation time  $T_{2b}$  and surface-relaxivity  $\rho$ ). For the former,  $1/T_2 = 1/T_{2b} + \rho S/V$ . We use  $T_{2b} = 3s$  for all simulations. Examples are given in Fig. 2

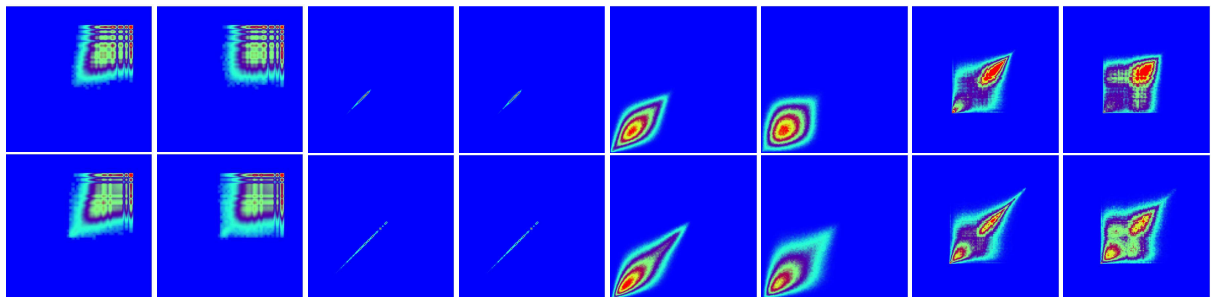


**Fig. 2:** Exchange plots for NZ sand (*top*) and Mt. Gambier limestone (*bottom*), with  $t_E = 100ms$  in pairs of two exchange times  $t_D = \{3;300\}$  ms. From left to right:  $T_2$ - $T_2$  from NMR simulation,  $d_{vs}$ - $d_{vs}$ ,  $d_{EDM}$ - $d_{EDM}$ ,  $T_{2CDM}$ - $T_{2CDM}$ . Axes are logarithmic (pairs from left to right) in [3;300]ms, [3.36;1680] $\mu$ m, [3.36;1680] $\mu$ m, [0.01;10]s.

### 2.3 Comparison to Experiment

The experimental  $T_2$ - $T_2$  plots (Fig. 3), see [10] for the pulse sequence, show exchange between different  $T_2$  environments. In the simulations we generate stronger exchange peaks when the  $T_2$  calculation is based on the covering radius map. A standard  $T_2$  simulation with constant  $\rho$  leads to weak exchange, while basing the exchange on pore partitions leads to no exchange.

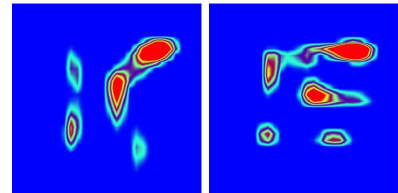


**Fig. 3:** Exp. NZ sand  $T_2$ - $T_2$  exchange plots,  $t_E = 50$  ms (right), 550 ms (left). Axes are logarithmic over the interval [3;300] ms.

### 3. Discussion and Conclusions

Exchange peaks are seen experimentally for the NZ sample, but not in the simulations using pore partitions, suggesting that there is no exchange between pores. When basing  $T_2$  relaxation times on the CRM, exchange peaks appear. Since the pore partition is using throats without volume (surfaces), it is plausible that the experiment measures exchange between pore bodies and either throats or crevices. It then appears that for smaller scale porosity exchange should really be measurable between pores itself. For small scale porosity ( $\approx 2 \mu\text{m}$ ), current Xray-CT technology reaches the resolution limit. To assign transport properties for regions of the image with unresolved porosity it would be desirable to use NMR spectral data in addition, leading to more accurate calculations of transport properties.

### References

- [1] K.R. Brownstein, C.E. Tarr, Phys. Rev. A 19 (1979), 2446-2453.
- [2] M.H. Cohen, K.S. Mendelson, J. Appl. Phys. 53 (1982), 1127-1135.
- [3] W.E. Kenyon, P. Day, C. Straley, J. Willemsen, Soc. Petr. Eng. 15643.
- [4] P.N. Sen, C. Straley, W.E. Kenyon, M.S. Whittingham, Geophysics 55 (1990), 61-69.
- [5] Y.-Q. Song, S. Ryu, P.N. Sen, Nature 406 (2000), 178-181.
- [6] K.R. McCall, D.L. Johnson, R.A. Guyer, Phys. Rev. B 44 (1991), 7344-7355.
- [7] S. Lonnes, A. Guzman-Garcia, R. Holland, Soc. Petr. & Well Log Analyst, 44<sup>th</sup> Annual Logging Symposium (2003), paper DDD.
- [8] K.E. Washburn, P.T. Callaghan, Phys. Rev. Lett. 97 (2006), 175502.
- [9] K.E. Washburn, P.T. Callaghan, J. Magn. Res. 186 (2007), 337-340.
- [10] K.E. Washburn, C.H. Arns, P.T. Callaghan, Phys. Rev. E 77 (2008), 051203.
- [11] L. Monteilhet, J. Korb, J. Mitchell, P. McDonald, Phys. Rev. E 74 (2006), 061404.
- [12] C.H. Arns, M.A. Knackstedt, W.V. Pinczewski, K.R. Mecke, Phys. Rev. E 63 (2001), 31112.
- [13] C.H. Arns, A. Sakellariou, T.J. Senden, A.P. Sheppard, R. Sok, W.V. Pinczewski, M.A. Knackstedt, Petrophysics 46 (2005), 260-277.
- [14] C.H. Arns, M.A. Knackstedt, N. Martys, Phys. Rev. E 72 (2005), 046304.
- [15] C.H. Arns, A.P. Sheppard, R.M. Sok, M.A. Knackstedt, Petrophysics 48 (2007), 202-221.
- [16] C.H. Arns, A.P. Sheppard, M. Saadatfar, M.A. Knackstedt, Soc. Petr. & Well Log Analyst, 47<sup>th</sup> Annual Logging Symposium (2006), paper GG.
- [17] A. Sakellariou, T.J. Sawkins, T.J. Senden, A. Limaye, Physica A 339 (2004), 152-158.
- [18] A.P. Sheppard, R.M. Sok, H. Averdunk, Physica A 339 (2004), 145-151.

### Acknowledgements

The authors are grateful for the X-ray CT data acquisition and phase segmentation performed by T.J. Senden and A.P. Sheppard. The authors acknowledge the Royal Society of New Zealand Marsden fund and the Australian Research Council for financial support. CHA thanks the Australian Research Council for an Australian Research Fellowship (DP0881112).